Changing recruitment capacity in global fish stocks

Gregory L. Britten[a,b,1], Michael Dowd[c], and Boris Worm[a]

[a]Department of Biology, Dalhousie University, Halifax, NS, Canada, B3H 4R2; [b]Department of Earth System Science, University of California, Irvine, CA 92697; and [c]Department of Mathematics and Statistics, Dalhousie University, Halifax, NS, Canada, B3H 4R2

Edited by James A. Estes, University of California, Santa Cruz, CA, and approved November 3, 2015 (received for review March 7, 2015)

Marine fish and invertebrates are shifting their regional and global distributions in response to climate change, but it is unclear whether their productivity is being affected as well. Here we tested for time-varying trends in biological productivity parameters across 262 fish stocks of 127 species in 39 large marine ecosystems and high-seas areas (hereafter LMEs). This global meta-analysis revealed widespread changes in the relationship between spawning stock size and the production of juvenile offspring (recruitment), suggesting fundamental biological change in fish stock productivity at early life stages. Across regions, we estimate that average recruitment capacity has declined at a rate approximately equal to 3% of the historical maximum per decade. However, we observed large variability among stocks and regions; for example, highly negative trends in the North Atlantic contrast with more neutral patterns in the North Pacific. The extent of biological change in each LME was significantly related to observed changes in phytoplankton chlorophyll concentration and the intensity of historical overfishing in that ecosystem. We conclude that both environmental changes and chronic overfishing have already affected the productive capacity of many stocks at the recruitment stage of the life cycle. These results provide a baseline for ecosystem-based fisheries management and may help adjust expectations for future food production from the oceans.

fisheries | population dynamics | productivity | recruitment | nonstationary processes

Human well-being is closely linked with the productivity of marine fisheries, which provide a significant source of protein for more than half of the world's population (1). However, ongoing environmental and biological changes may impact productivity through a variety of mechanisms, including larger habitat areas for temperate species (2), altered body sizes (3), food availability (4), and increased exposure to oxygen-depleted and acidic waters (5). Recent research has documented marked changes in the distributional patterns of marine species that are consistent with climate forcing (6, 7). However, the net effect of these changes on global fish stock productivity is not clearly understood. In particular, documented environmental changes (4, 8, 9) and the long-term consequences of overfishing (10, 11) all impose relevant but poorly constrained effects. Here we help address this issue by evaluating the evidence for empirical trends in the relation between the size of the reproductively mature population (or "spawning stock") and the annual production of juvenile offspring ("recruits") using a recently synthesized global database of stock-recruit time series (12). We then test the relation between empirical recruitment trends and regional environmental variables associated with temperature, phytoplankton abundance, and historical overfishing.

Recruitment is modeled by relating the size of the spawning stock biomass to the annual production of recruits. The magnitude of annual recruitment is highly variable (13), yet it provides the basis for population growth and stock productivity by determining the initial number of fish that may grow, die, or be harvested by the fishery (14) (i.e., total productivity is the combination of recruitment, individual growth, and mortality). As such, the stock-recruit relationship has been identified as "the most important and generally most difficult problem in the biological assessment of fisheries" (14). The simplest commonly used recruitment function is the Ricker model

$$R_t = \alpha B_{t-\tau} e^{-\beta B_{t-\tau}},$$

where recruitment R at time t is an increasing function of the spawning stock biomass B (lagged by the age of recruitment τ), with negative exponential density-dependent feedback. The two model parameters, α and β, characterize the magnitude of recruitment, where α is the maximum reproductive rate (or density-independent recruitment), and β gives the rate at which recruitment is reduced by density-dependent feedbacks. These two parameters combine to give the maximum recruitment capacity for an individual stock when $dR/dB = 0$ and $(d^2R)/(dB^2) < 0$, yielding

$$\mathrm{R_{MAX}} = \frac{\alpha}{\beta} e^{-1},$$

where e is Euler's number. Note that $\mathrm{R_{MAX}}$ is a biomass-independent measure of maximum recruitment and does not depend on current stock size. This property of the measure is attractive as it allows comparison of both abundant and heavily depleted stocks, but it also means that $\mathrm{R_{MAX}}$ occasionally occurs at biomass levels larger than those observed today. Because $\mathrm{R_{MAX}}$ is highly correlated with alternative biomass-dependent measures of recruitment success (*SI Appendix*), we adopt it as a simple and comparable metric of fish stock productivity at the recruitment stage of their life cycle.

Results

When recruitment models are fitted to data (Fig. 1 *A*–*F*), there is often considerable structure in the residual variation (Fig. 1 *G*–*I*) that suggests that biological productivity may have changed significantly over time. Trends can be observed as directed declines (Fig. 1*G*), threshold-like dynamics (Fig. 1*H*), or regime shifts (Fig. 1*I*; note that the observed shift coincided with the 1977 reversal of the Pacific Decadal Oscillation) (15). We evaluated evidence for

Significance

Marine fish stocks play an important role in marine ecosystems and provide a source of protein for billions of people worldwide. Recent environmental changes have affected the distribution of many stocks, but it is yet unclear whether their productivity is affected as well. We show that recruitment capacity (the ability of stocks to produce surviving offspring) has been significantly altered by both environmental changes and biological changes brought about by overfishing. In total, these effects have reduced recruitment capacity by 3% of the historical maximum per decade, on average. This paper helps us to understand and track previously unrecognized changes in fish stock productivity during the early stages of their life cycle.

Author contributions: G.L.B., M.D., and B.W. designed research; G.L.B. performed research; G.L.B. analyzed data; and G.L.B., M.D., and B.W. wrote the paper.

The authors declare no conflict of interest.

This article is a PNAS Direct Submission.

[1]To whom correspondence should be addressed. Email: gbritten@uci.edu.

This article contains supporting information online at www.pnas.org/lookup/suppl/doi:10.1073/pnas.1504709112/-/DCSupplemental.

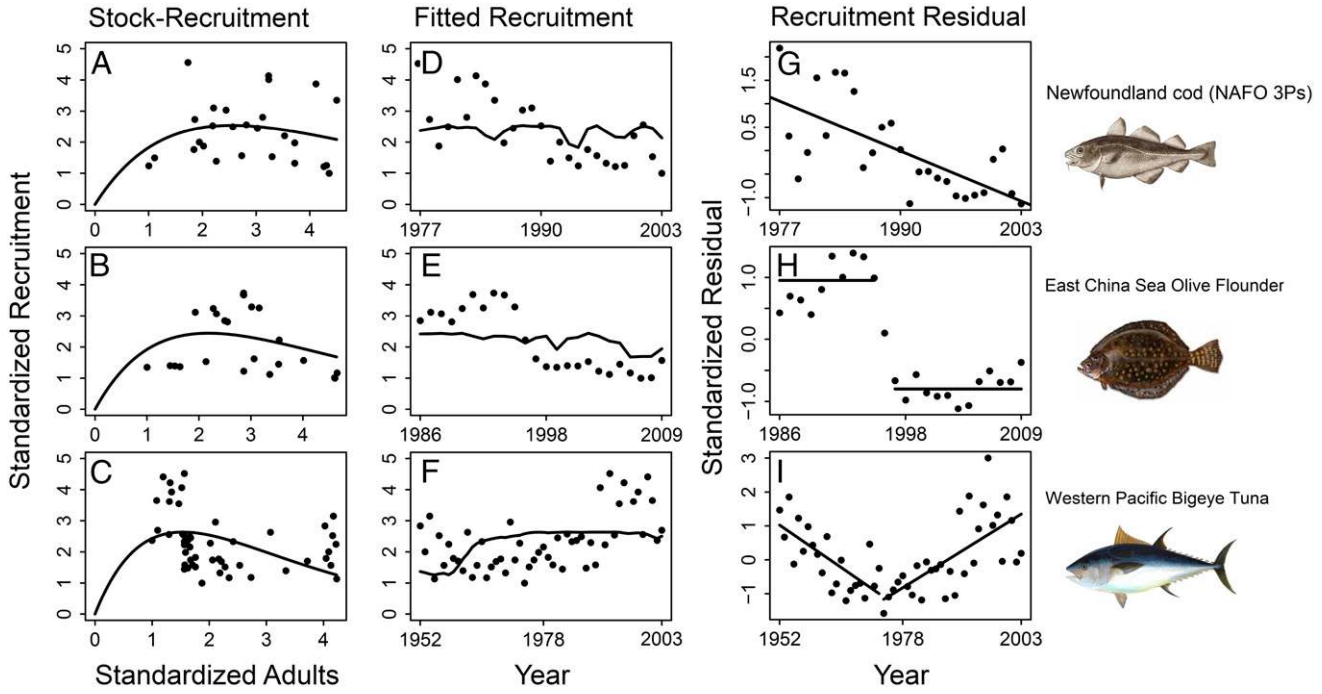

Fig. 1. Patterns in stock-recruitment data. Ricker models fitted to stock-recruitment data (*A*–*C*) often display systematic errors (*D*–*F*). Model residuals can show diverse behaviors, including progressive declines (*G*), abrupt thresholds (*H*), or reversing regime shifts (*I*). Data are standardized to have unit variance.

changes in recruitment by performing model selection with respect to static or time-varying biological parameters within the Ricker model (i.e., α and β; *Methods*) and estimated changes through time where parameters are indeed found to vary. We then summarized trends in recruitment as follows. For an individual stock, we computed the linear slope of R_{MAX} with respect to time (denoted ΔR_{MAX}) and standardized the slopes to have units of percent change per decade relative to the stock-specific historical maximum, thus combining effects of α and β and capturing broad-scale trends through time. To describe trends across stocks, we combined ΔR_{MAX} estimates using random-effects meta-analysis to control for variable time series length and goodness-of-fit across individual stocks. We denote meta-analytic averages ΔR^k_{MAX}, representing the mean ΔR_{MAX} for a group k. Groupings are made on basis of individual large marine ecosystems (LMEs) and major taxonomic groups. We adopt the LME definition as a simple, ecologically meaningful (16) and management-relevant (17) way to spatially categorize individual stocks. To relate recruitment trends to the environment, we use multiple regression to model ΔR^k_{MAX} as a function of estimated linear changes in sea surface temperature (denoted ΔSST), chlorophyll concentration (ΔCHL, a widely-used a proxy of phytoplankton standing stock), and a measure of historical overfishing (taken as the average ratio of historical stock biomass to target biomass, denoted $B{:}B_{MSY}$). Environmental variables ΔSST and ΔCHL were computed from quality-controlled, publically available databases consistent with the time window covered by stock assessments within individual LMEs, and $B{:}B_{MSY}$ was calculated as the mean values across all stocks within each LME. See *Methods* and *SI Methods* for full details.

We found that stock-recruitment data supported time-varying recruitment capacity (R_{MAX}) for 71% (n = 186) of stocks according to model selection (Fig. 2). Of these, 69% (n = 128) showed negative trends (Fig. 2). For all stocks combined, ΔR^k_{MAX} was estimated at approximately −3% per decade, relative to the historical maximum ($P < 0.001$; Fig. 2*D*). However, there was a broad-scale divergence in values between the North Pacific and North Atlantic oceans, with the North Atlantic showing steeper declines. In contrast, the North Pacific showed approximately neutral trends across four LMEs, each with a relatively large number of stocks. Across all LMEs, we estimated that 31 of all 39 LMEs (79%), and 20 of 27 LMEs with more than three assessed stocks (74%), showed negative ΔR^k_{MAX} (Fig. 2). The most positive value was found in the Gulf of Mexico, whereas the heavily depleted Newfoundland and Labrador LME showed the most negative trend (Fig. 2*B*).

There was significant variation associated with different taxa. Groundfish (bottom-associated species such as flatfishes, Pleuronectiformes, and cod-like Gadiformes) showed the most negative ΔR^k_{MAX} (Fig. 2*C*). At the species level, the most negative values were observed for several North Atlantic species such as American plaice (*Hippoglossoides platessoides*), European plaice (*Pleuronectes platessa*), common European sole (*Solea vulgaris*), and Atlantic cod (*Gadus morhua*). In the North Pacific, however, many groundfish species showed opposite patterns, with stocks of rex sole (*Glyptocephalus zachirus*), flathead sole (*Hippoglossoides elassodon*), and arrowtooth flounder (*Atheresthes stomias*) trending positively. Pelagic (open-water) species such as herring (*Clupea harengus, C. pallasii*) and swordfish (*Xiphias gladius*) often showed ΔR^k_{MAX} values closer to zero.

In general, we found individual stock-recruit parameters changed in a way that resulted in stronger density-dependent processes and reduced maximum reproductive rates. Of individual stocks with negative ΔR_{MAX}, 71% displayed more negative β parameters and 29% experienced declining α, according to model selection. We also performed the analysis over a fixed common time window (1980–2000) and found that the two ΔR_{MAX} values correlated strongly ($r = 0.82$; $P < 0.001$), suggesting that the observed trends are robust to stocks having variable time series length. We also found that ΔR_{MAX} was generally independent of the assumed form of density dependence in the stock-recruit model or to whether the model let α or β vary in time, indicating further robustness in ΔR_{MAX}. Likewise, using an alternative metric of recruitment success (expected recruitment at the median historically

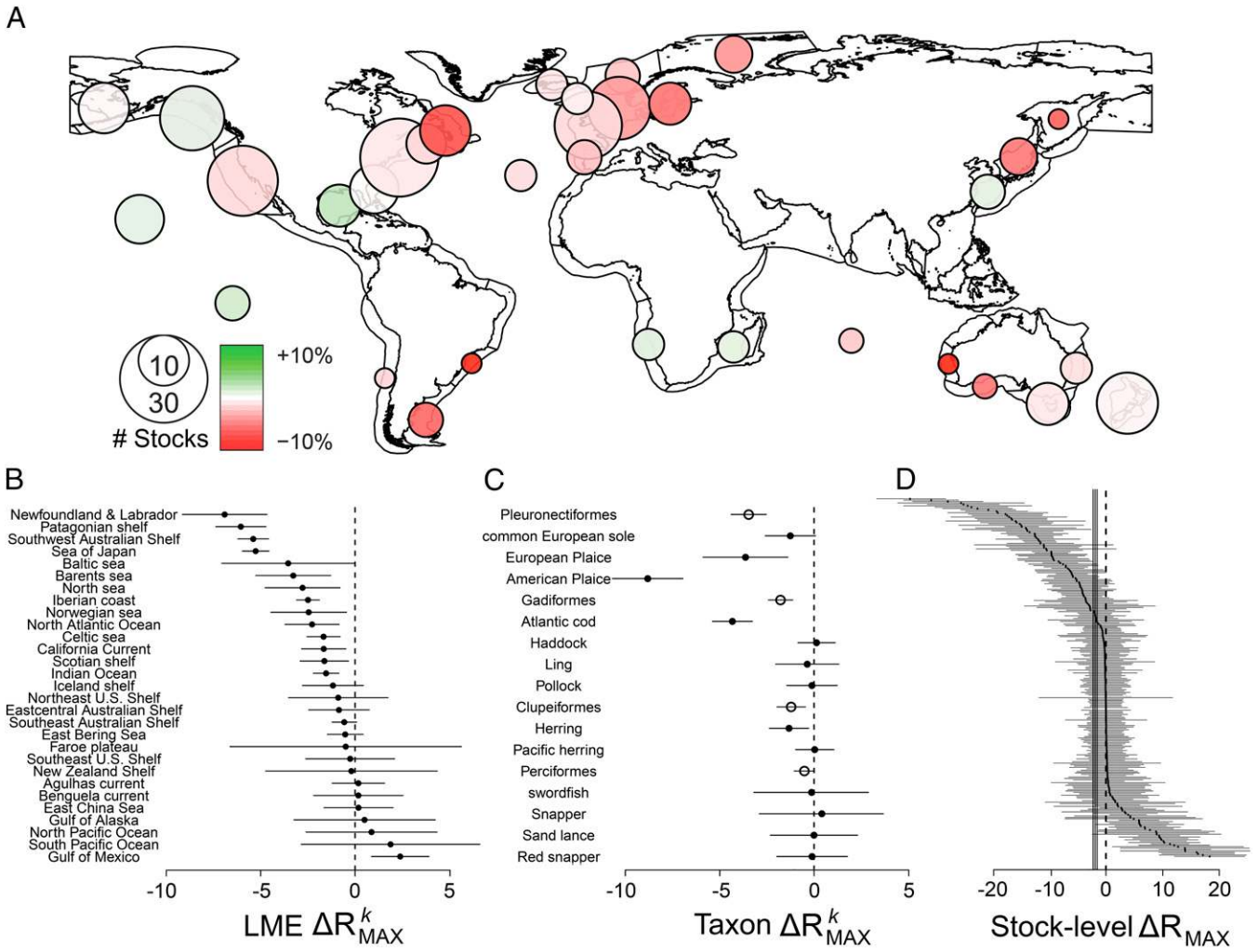

Fig. 2. Meta-analysis. Standardized trends in recruitment capacity (ΔR_{MAX}; units % change R_{MAX} per decade, relative to the historical maximum) estimated by changes in biological recruitment parameters (see text). (*A*) ΔR^k_{MAX} (representing the meta-analytic average ΔR_{MAX}) by LME containing more than three assessed stocks. The color of the circle gives the direction and magnitude of ΔR^k_{MAX} and the size of the circle gives the number of stocks in the LME. (*B*) Meta-analytic ΔR^k_{MAX} per LME and SE. (*C*) Taxon-level ΔR^k_{MAX} for species with more than three assessed stocks (●) and by taxonomic order (○). (*D*) All 262 individual stock ΔR_{MAX} with the grand meta-analytic mean ($P < 0.001$) and SE (shaded bar). Meta-analytic means were derived by averaging the individual stock trends by inverse-variance weighting.

observed biomass) we found no major change in the resulting trends (see *SI Methods* for details on these sensitivity analyses).

Importantly, average trends in recruitment capacity in each ecosystem were found to be significantly related to environmental and fishing-related variables (ΔCHL and $B:B_{MSY}$) across all LMEs (Fig. 3). Considering all species together (Fig. 3*A*), ΔR^k_{MAX} in each LME was positively associated with ΔCHL (Fig. 4*A*), which accounted for 38% of the total variance. Again, an interesting contrast emerged when isolating the heavily exploited groundfish (combining orders Pleuronectiformes and Gadiformes; Fig. 3*B*). Here, the history of overfishing emerged as the most important predictor and explained 58% of the total variance. Analysis of the pelagic Perciformes and Clupeiformes revealed a positive effect of ΔCHL and negative effect of ΔSST, but these were marginally insignificant. We also investigated patterns of recruitment variation with respect to maximum body size but found no significant relationships.

Discussion

Taken together, these results provide empirical context for understanding contemporary changes in the productivity of exploited marine fish stocks. To date, future forecasts of fisheries productivity have varied in their predictions; for example, the productivity of temperate species has been projected to increase 30–40% based on expansion of fish habitat and increased primary productivity (2), whereas models of individual fish metabolism predict shrinking body sizes with warming oceans (3) that could affect fecundity and productivity. A recent global study of fisheries time series demonstrated that the relationship between adult biomass and total yield can be highly nonstationary (18), but the forcing of such changes has remained unclear. Here we focused our empirical analysis on stock recruitment dynamics and related observed nonstationary patterns to changes in plankton abundance and the history of overfishing. The observed changes in productivity at the recruitment stage of the life cycle may provide a partial explanation for nonstationary patterns observed in fisheries yield for the affected stocks.

We caution that these trends in recruitment biology represent broad-scale spatial and temporal patterns when averaging over many stocks and regions. These patterns should be combined with other model-based forecasts that weigh factors related to habitat quantity and quality to more fully determine expected change in

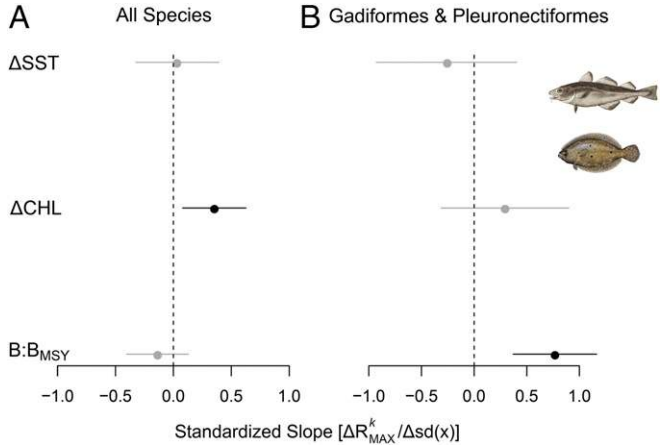

Fig. 3. Drivers of recruitment capacity. Relationships between LME-level ΔR^{k}_{MAX} and environmental and fisheries variables for all species (*A*) and orders Gadiformes and Pleuronectiformes (*B*) using multiple regression (weighted according to the number of stocks in the LME). The three LME-specific covariates tested include (*i*) observed changes in average sea surface temperature (ΔSST) and (*ii*) chlorophyll concentration (ΔCHL), as well as changes in overfishing indicated by the ratio of observed to target biomass ($B:B_{MSY}$). See Fig. 4 for spatial patterns. The regression slopes were normalized by transforming the regression variables to unit variance. Black symbols indicate statistical significance. See text and *SI Methods* for details.

biomass distribution and the productivity of individual stocks. We further note that the drivers of recruitment capacity identified here likely vary in importance among stocks and regions. Bottom-up changes in plankton concentration and top-down effects of overfishing are all known to affect recruitment in complex ways, including effects at both the adult (e.g., maternal effects on recruitment) (19) and larval stages (e.g., food availability) (20). Our results, however, make neither assumptions nor inferences regarding stock-specific mechanisms. Finally, correlations in recruitment may also be important for inferring long-term trends and patterns of shared responses to environmental changes and fishing at the regional scale. We emphasize that a more detailed hierarchical approach that accounts for recruitment correlations (21, 22) and species interactions is needed to fully resolve regional patterns and drivers and thus provide direct management guidance for individual stocks within individual LMEs.

At larger scales, the apparent divergence in productivity among the North Pacific and North Atlantic provides an interesting contrast, possibly linked to divergent ecological histories. The North Pacific experienced a large oceanographic regime shift in the 1970s (15), which resulted in relatively flat long-term environmental trends (Fig. 4). Observed patterns suggest that recruitment capacity may have tracked this variability (Fig. 1*I*), resulting in small ΔR^{k}_{MAX} values overall. Shorter histories of exploitation and lower exploitation rates (23) are also likely to have tempered declines in this region due to overfishing. In contrast, the North Atlantic is marked by strong directional environmental change and long-term overexploitation (Fig. 4). Environmental and fishing-related trends in this region were among the most severe and were significantly related to observed changes in recruitment capacity. An exception for the North Atlantic trend is the positive ΔR^{k}_{MAX} value in the Gulf of Mexico [12 of 13 time series there predate the *Deepwater Horizon* (24) spill in 2010]. It is also important to note that the database is most representative of North American and European stocks due to the relative scarcity of stock assessments in tropical oceanic regions of the world (Fig. 4*C*) (12, 25) where earth system models predict that plankton productivity will decline more strongly than in the coastal and temperate regions that dominate the stock recruitment database (26). This historical bias in spatial coverage limits our understanding of global fish populations as a whole (25).

In addition to impacting the productivity of marine fish stocks, observed changes in recruitment parameters may also have consequences for the stability of populations. Recent theoretical work has linked observed patterns of population stability (27) to changes in stock recruitment parameters (28) due to age-selective fishing. It was hypothesized that population stability has decreased in stocks due to increases in the mean and variance of the maximum reproductive rate α caused by the truncation of population age structure by fishing. Our results, however, suggest that such increases in α are not often observed in assessed fish populations, where α has generally trended downward. Rather, frequently observed increases in the magnitude of the density-dependent parameter β may provide an alternative explanation for reduced stability in exploited stocks based on the well-known destabilizing effects of strong density-dependent feedbacks (29). Testing this hypothesis should be a priority for follow-up research.

In summary, empirically estimated trends in recruitment capacity (Figs. 1 and 2) provide evidence for environmental- and fishing-related changes in the productivity of marine fish stocks (Fig. 3). Although far from uniform at the stock level, observed trends were significantly related to ongoing environmental and biological change at the ecosystem scale, specifically changes in phytoplankton biomass and the history of stock biomass depletion (Fig. 4 *B* and *C*). The reality of time-varying biological parameters requires managers to revisit the common assumptions of fixed maximum sustainable yields (30) and emphasizes the need for ecosystem-based management strategies that investigate and account for observed environmental and fishing-related impacts on the long-term productive capacity of fish stocks. Such strategies are enabled by the methods presented here, in that the complex effects of environmental changes can be tracked within a reasonably simple assessment framework. Accounting for such changes is a prerequisite for the successful rebuilding and sustainable harvesting of fisheries resources in a rapidly changing environment.

Methods

The RAM Legacy Stock Assessment Database. All stock recruitment data were extracted from the RAM Legacy Stock Assessment Database (12), which is a global, quality-controlled database, available publicly at ramlegacy.org/. Stock assessments provide estimates of both spawning stock biomass (kilograms) and recruitment (no. individuals). We analyzed 262 of the ∼420 time series available in the database based on (*i*) whether a recruitment relationship was already assumed in generating the stock assessment estimates (12) and (*ii*) whether the spawning stock biomass and recruitment time series were estimated directly, as opposed to indirect proxies such as spawner egg abundance. All series were then normalized to unit variance for easy comparison across stocks and regions. A list of species used in the analysis, along with their designated LME, can be found in Table S1. Frequency histograms of the start and end dates of the stock recruitment time series are shown in Fig. S1 and tabulated in Table S2.

Nonstationary Recruitment Model. The Ricker model can be linearized by reexpressing recruitment as log survival

$$\ln\left(\frac{R_t}{B_{t-\tau}}\right) = \ln\alpha - \beta B_{t-\tau}.$$

This model can be fitted to data as a linear regression. To model nonstationary recruitment relationships, we let the recruitment parameters vary in time (21, 31) by specifying the following linear Gaussian state space model

$$\ln\left(\frac{R_t}{B_{t-\tau}}\right) = \ln\alpha_t - \beta_t B_{t-\tau} + w_t, \qquad w_t \sim \mathrm{N}(0, \sigma_o^2),$$

$$\begin{bmatrix}\ln\alpha\\ \beta\end{bmatrix}_t = \begin{bmatrix}\ln\alpha\\ \beta\end{bmatrix}_{t-1} + \begin{bmatrix}v_1\\ v_2\end{bmatrix}_t, \qquad \begin{bmatrix}v_1\\ v_2\end{bmatrix}_t \sim \mathbf{N}\left(\begin{bmatrix}0\\ 0\end{bmatrix}, \mathbf{Q} = \begin{bmatrix}\sigma^2_{\ln\alpha} & 0\\ 0 & \sigma^2_{\beta}\end{bmatrix}\right),$$

where the recruitment parameters are treated as dynamic latent states. Note that w_t is the observation error with variance σ_o^2 and $[v_1\ v_2]_t'$ is the process

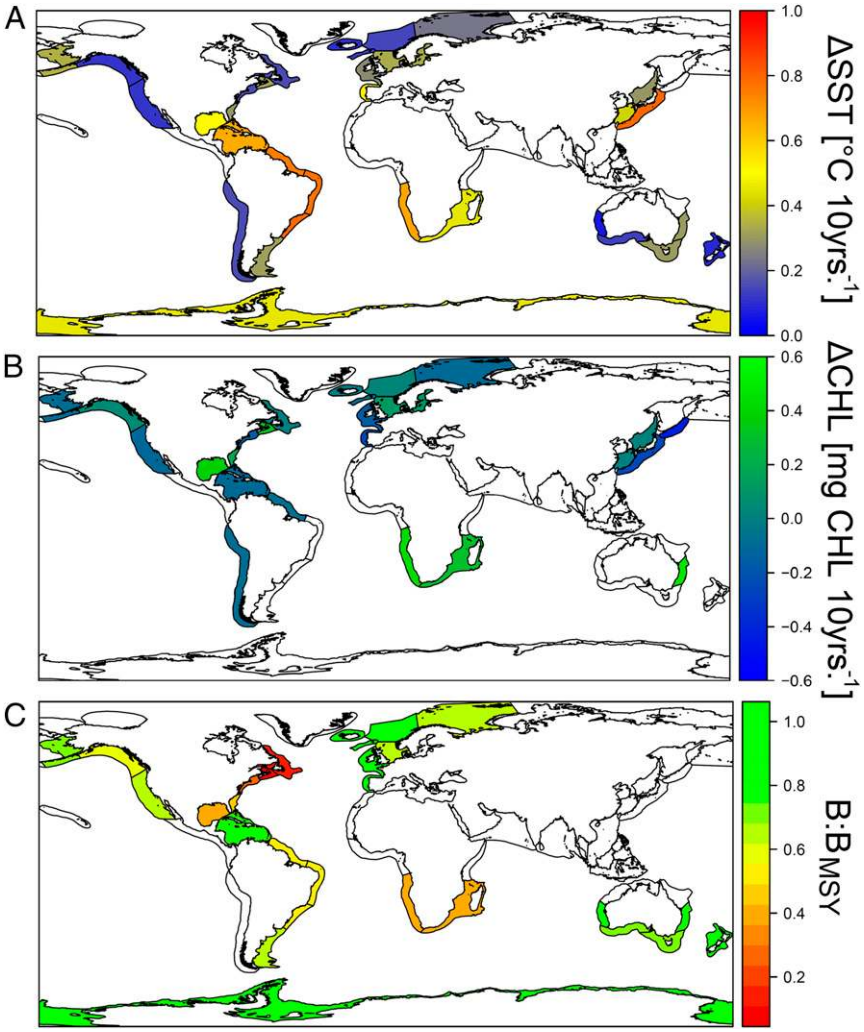

Fig. 4. Spatial distribution of environmental variables by LME. (*A*) ΔSST computed over the period covered by stock assessments in each LME. (*B*) ΔCHL (used as a common proxy for phytoplankton biomass). (*C*) $B:B_{MSY}$ (12).

error vector with covariance matrix **Q**. The unknown parameters are σ_o^2 and the diagonal of the matrix **Q**, which are estimated by the method of maximum likelihood. Details of the estimation can be found in *SI Methods*, including the model selection algorithm based on the Bayesian information criterion (BIC). Model selection was used to determine whether variance parameters should be zero or nonzero, thus determining whether the data support static or time-varying recruitment parameters (*SI Methods*). For stocks with at least one time-varying parameter, the trend in R_{MAX} was summarized by a linear slope (ΔR_{MAX}) standardized to have unit percent change per decade relative to the historical maximum. For stocks where both α and β were inferred as static, ΔR_{MAX} is zero. Results for the time-varying recruitment analysis for all stocks, along with statistical diagnostics, are displayed in *SI Appendix*. Model selection results are also given in Table S3.

Meta-Analysis. The nonstationary recruitment analysis and subsequent trend analysis were applied to each stock individually, and then regional and taxonomic patterns were summarized using a random effects meta-analysis model. The random effects model is written

$$\Delta R^i_{MAX} = \Delta R^k_{MAX} + \vartheta^i + \varphi^i,$$

where ΔR^i_{MAX} is the linear slope of R_{MAX} for stock i, ΔR^k_{MAX} is the overall mean across all stocks in group k, ϑ^i is the deviation of the observed ΔR^i_{MAX} from the "true" ΔR^i_{MAX}, and φ^i is the deviation of the true ΔR^i_{MAX} from ΔR^k_{MAX}. The random effects analysis assumes that a group trend can be described by an inverse-variance weighted average of trends across stocks and stock-specific deviations from the overall trend (*SI Methods*). The meta-analysis model was implemented in the R package *rmeta* (32). All meta-analytic results for LMEs and taxa are given in the *SI Appendix*, which gives group-specific slopes and contributions from individual stocks. Three sensitivity analyses were also performed and are documented in *SI Methods*. These analyses included robustness tests against (*i*) alternative forms of density dependence (Figs. S2–S4); (*ii*) BIC model selection algorithm (Fig. S5); (*iii*) the choice of alternative metrics of recruitment success (Fig. S6); and (*iv*) the impact of variable time series length (Fig. S7).

Global Scale Correlates of Recruitment. To correlate recruitment trends to environmental change and overfishing intensity, we fit multiple regression models of the form

$$\Delta \mathbf{R}^k_{\mathbf{MAX}} = c_0 + c_1 \Delta SST + c_2 \Delta CHL + c_3 B:BMSY + e_k,$$

where $\Delta \mathbf{R}^k_{\mathbf{MAX}}$ is the vector of ΔR^k_{MAX} estimated per LME, ΔSST is the linear trend in sea surface temperature in each LME, ΔCHL is the linear trend in chlorophyll concentration (a widely used proxy for phytoplankton biomass), $B:B_{MSY}$ is an index of historical overfishing, representing the mean historical ratio of annual biomass to target biomass levels as extracted from the stock assessments (12), c_0 is the intercept, c_1, c_2, c_3 are the partial slopes, and e_k is the LME-specific regression error. ΔSST and ΔCHL were computed according to the time window covered by stock assessments within individual LMEs. The frequency distributions of time series start and end dates are shown in Fig. S1. Historical SST data were extracted from the Simple Ocean Data Assimilation (33), and CHL data were taken from the in situ database provided in ref. 8. The trend model for CHL contained a seasonal term due to unequal seasonal sampling, whereas mean annual temperatures were extracted for SST. The

regression was weighted according to the number of stocks in each LME. We tested possible interactions but none were retained. All independent variables were standardized to unit variance to standardize the regression coefficients.

The multiple regression analysis was fit three times on three sets of species. The first included all species in each LME, and two more subsets (within LMEs) were made on the basis of taxonomic order. One taxonomic grouping included Gadiformes and Pleuronectiformes (generally bottom-associated species) and other included Clupeiformes and Perciformes (pelagic, open-water species). These orders do not occur in all LMEs; therefore, the regression analysis on the subsets included fewer data points. The Gadiformes and Pleuronectiformes occurred in 21 LMEs and the Perciformes and Clupeiformes occurred in 23 LMEs.

ACKNOWLEDGMENTS. We thank all the stock assessment scientists whose dedicated work made this research possible. We also thank C. Minto, R. Mohn, D. Ricard, J. Hutchings, J. Mills-Flemming, and S. Ambrose for discussions; D. Hively, R. Hilborn, and D. Boyce for data; S. Ambrose for data processing; and four anonymous reviewers whose suggestions strengthened the paper. We gratefully acknowledge the Natural Sciences and Engineering Research Council of Canada and the Sobey Fund for Oceans for funding.

1. FAO (2012) *The Status of World Fisheries and Aquaculture* (United Nations Food And Agriculture Organisation, Rome).
2. Cheung WWL, et al. (2010) Large-scale redistribution of maximum fisheries catch potential in the global ocean under climate change. *Glob Change Biol* 16(1):24–35.
3. Cheung WWL, et al. (2012) Shrinking of fishes exacerbates impacts of global ocean changes on marine ecosystems. *Nat Clim Chang* 3(3):254–258.
4. Boyce DG, Dowd M, Lewis MR, Worm B (2014) Estimating global chlorophyll changes over the past century. *Prog Oceanogr* 122(1):163–173.
5. Mora C, et al. (2013) Biotic and human vulnerability to projected changes in ocean biogeochemistry over the 21st century. *PLoS Biol* 11(10):e1001682.
6. Pinsky ML, Worm B, Fogarty MJ, Sarmiento JL, Levin SA (2013) Marine taxa track local climate velocities. *Science* 341(6151):1239–1242.
7. Cheung WWL, Watson R, Pauly D (2013) Signature of ocean warming in global fisheries catch. *Nature* 497(7449):365–368.
8. Boyce DG, Lewis M, Worm B (2012) Integrating global chlorophyll data from 1890 to 2010. *Limnol Oceanogr Methods* 10(11):840–852.
9. Belkin IM (2009) Rapid warming of large marine ecosystems. *Prog Oceanogr* 81(4): 207–213.
10. Conover DO, Munch SB (2002) Sustaining fisheries yields over evolutionary time scales. *Science* 297(5578):94–96.
11. Olsen EM, et al. (2004) Maturation trends indicative of rapid evolution preceded the collapse of northern cod. *Nature* 428(6986):932–935.
12. Ricard D, Minto C, Jensen OP, Baum JK (2012) Examining the knowledge base and status of commercially exploited marine species with the RAM Legacy Stock Assessment Database. *Fish Fish* 13(4):380–398.
13. Thorson JT, Jensen OP, Zipkin EF (2014) How variable is recruitment for exploited marine fishes? A hierarchical model for testing life history theory. *Can J Fish Aquat Sci* 71(7):973–983.
14. Hilborn R, Walters CJ (1992) *Quantitative Fisheries Stock Assessment: Choice, Dynamics and Uncertainty* (Chapman and Hall/CRC, New York).
15. Mantua N, Hare SR, Zhang Y, Wallace JM, Francis RC (1997) A Pacific interdecadal climate oscillation with impacts on salmon production. *Bull Am Meterological Soc* 78(6):1069–1079.
16. Sherman K (1991) The Large Marine Ecosystem concept: Research and management strategy for living marine resources. *Ecol Appl* 1(4):350–360.
17. Fanning L, et al. (2007) A large marine ecosystem governance framework. *Mar Policy* 31(4):434–443.
18. Vert-pre KA, Amoroso RO, Jensen OP, Hilborn R (2013) Frequency and intensity of productivity regime shifts in marine fish stocks. *Proc Natl Acad Sci USA* 110(5):1779–1784.
19. Shelton AO, Munch SB, Keith D, Mangel M (2012) Maternal age, fecundity, egg quality, and recruitment: Linking stock structure to recruitment using an age-structured Ricker model. *Can J Fish Aquat Sci* 69(10):1631–1641.
20. Platt T, Fuentes-Yaco C, Frank KT (2003) Marine ecology: Spring algal bloom and larval fish survival. *Nature* 423(6938):398–399.
21. Minto C, Flemming JM, Britten GL, Worm B (2014) Productivity dynamics of Atlantic cod. *Can J Fish Aquat Sci* 71(2):203–216.
22. Thorson JT, Stewart IJ, Taylor IG, Punt AE (2013) Using a recruitment-linked multispecies stock assessment model to estimate common trends in recruitment for US West Coast groundfishes. *Mar Ecol Prog Ser* 483(1):246–256.
23. Worm B, et al. (2009) Rebuilding global fisheries. *Science* 325(5940):578–585.
24. McCrea-Strub A, et al. (2011) Potential impact of the deepwater horizon oil spill on commercial fisheries in the Gulf of Mexico. *Fisheries* 36(7):332–336.
25. Costello C, et al. (2012) Status and solutions for the world's unassessed fisheries. *Science* 338(6106):517–520.
26. Bopp L, et al. (2013) Multiple stressors of ocean ecosystems in the 21st century: Projections with CMIP5 models. *Biogeosciences* 10(10):6225–6245.
27. Anderson CNK, et al. (2008) Why fishing magnifies fluctuations in fish abundance. *Nature* 452(7189):835–839.
28. Shelton AO, Mangel M (2011) Fluctuations of fish populations and the magnifying effects of fishing. *Proc Natl Acad Sci USA* 108(17):7075–7080.
29. Hassell MP (1975) Density-dependence in single-species populations. *J Anim Ecol* 44(1):283–295.
30. Walters CJ (1987) Nonstationarity of production realtionships in exploited populations. *Can J Fish Aquat Sci* 44(1):156–165.
31. Peterman RM, Pyper BJ, Macgregor BW (2003) Use of the Kalman filter to reconstruct historical trends in productivity of Bristol Bay sockeye salmon. *Can J Fish Aquat Sci* 824(7):809–824.
32. Lumley T (2012) rmeta: Meta-Analysis (CRAN, Vienna), R Package Version 2.16.
33. Carton JA, Giese BS (2008) A reanalysis of ocean climate using simple ocean data assimilation (SODA). *Mon Weather Rev* 136(8):2999–3017.
34. Durbin J, Koopman SJ (2008) *Time Series Analysis by State Space Methods* (Oxford Univ Press, Oxford).
35. Myers RA, Bowen KG, Barrowman NJ (1999) Maximum reproductive rate of fish at low population sizes. *Can J Fish Aquat Sci* 56(12):2404–2419.
36. Myers RA (2001) Stock and recruitment: Generalizations about maximum reproductive rate, density dependence, and variability using meta-analytic approaches. *ICES J Mar Sci* 58(5):937–951.
37. Myers RA, Barrowman NJ (1990) Time series bias in the estimation of density-dependent mortality in stock-recruitment models. *Can J Fish Aquat Sci* 52(1):223–232.

Supporting Information

Britten et al. 10.1073/pnas.1504709112

SI Methods

Here we provide additional detailed regarding the analysis. For compact description of the estimation, we define the recruitment parameter vector $\boldsymbol{\theta} = [\ln \alpha, \beta]'$. Thus, the linear Gaussian state space models can be written

$$y_t = \mathbf{H_t}\boldsymbol{\theta_t} + w_t \qquad w_t \sim N(0, \mathbf{R} = \sigma_o^2)$$

$$\boldsymbol{\theta_t} = \boldsymbol{\theta}_{t-1} + \mathbf{v_t} \qquad \mathbf{v_t} \sim \mathbf{N}\left(0, \mathbf{Q} = \begin{bmatrix} \sigma^2_{\ln\alpha} & 0 \\ 0 & \sigma^2_{\beta} \end{bmatrix}\right),$$

where y_t is the observed log survival at time t, $\mathbf{H_t}$ is the design matrix, w_t is a realization of the Gaussian observation error at time t with variance $\mathbf{R}$, and $\mathbf{v_t}$ is a realization of the bivariate Gaussian process error at time t with covariance $\mathbf{Q}$. Conditional on $\mathbf{R}$ and $\mathbf{Q}$ and initial values for the state vector $\boldsymbol{\theta}_0$, the optimal reconstruction for the latent time-varying recruitment parameters $\boldsymbol{\theta_t}$ are estimated using the Kalman filter and smoother (34). Note that variance parameters $\mathbf{R}$ and $\mathbf{Q}$ are estimated by maximum likelihood, whereas the recruitment parameters ($\boldsymbol{\theta_t}$) are analytically determined by the forward-filter/backward smoother Kalman smoother algorithm, conditional on $\mathbf{R}$, $\mathbf{Q}$, and $\boldsymbol{\theta}_0$ (the latter assumed to take the form of a diffuse Gaussian).

Maximum Likelihood Estimation. Maximum likelihood estimation (MLE) is based on the normally distributed one-step ahead prediction errors of the filtering algorithm (34), termed the innovations. The innovations for the dynamic regression are given by

$$\delta_t = y_t - \mathbf{H_t}\hat{\boldsymbol{\theta}}_\mathbf{t},$$

where $\hat{\boldsymbol{\theta}}$ denotes an estimate. The error covariance of the innovations is defined by

$$\mathbf{F_t} = \mathbf{H_t}\mathbf{M_t}\mathbf{H_t}' + \mathbf{R},$$

where $\mathbf{M_t}$ is the predictive covariance (34). The log likelihood of the innovations can then be written as

$$\text{Log L}(\mathbf{R}, \mathbf{Q}) = c - \frac{1}{2}\sum_{t=1}^{T} \ln|\mathbf{F_t}| - \frac{1}{2}\sum_{t=1}^{T} \delta_t'\mathbf{F_t}\delta_t,$$

where c is a constant. Log L is maximized using standard nonlinear optimization, yielding MLE estimates of $\mathbf{R}$, $\mathbf{Q}$, and subsequently $\hat{\boldsymbol{\theta}}_\mathbf{t}$ (hat denotes the MLE estimate) by applying the Kalman filter/smoother algorithm. All calculations were written in the R language (www.r-project.org), and the optimization was performed using the numerical routines within the R base package.

Model Selection. To determine whether individual recruitment time series have stationary or nonstationary parameters, we applied model selection using various parameterizations of the matrix $\mathbf{Q}$. We used the BIC for model selection, which is given as

$$\text{BIC} = -2\widehat{\text{Log}}\ \text{L} + k \ln T,$$

where $\widehat{\text{Log}}\ \text{L}$ is the optimized value of the log likelihood, k is number of nonzero estimable variance parameters in the dynamic regression model, and T is the length (number of years) of an individual recruitment time series. We consider four parameterizations of $\mathbf{Q}$ which represent (i) static stock-recruit relationship (all elements of $\mathbf{Q}$ equal to zero; $k = 1$); (ii) time-varying maximum reproductive rate, static density dependence [element (1,1) nonzero, all others zero; $k = 2$]; (iii) static maximum reproductive rate, time-varying density dependence [element (2,2) nonzero, all other zero; $k = 2$]; and (iv) time-varying maximum reproductive rate and density dependence [elements (1,1) and (2,2) nonzero, all others zero; $k = 3$]. Note we did not test the full covariance matrix with nonzero off-diagonal elements due to the inherent statistical dependency between the two stock-recruitment parameters (14). Under each parameterization, the Kalman filter/smoother algorithm yields a likelihood that can be used to compute the BIC. {Note that we adopt the BIC over the more common AIC to be more conservative in model selection in the sense that BIC favors fewer parameters due to its stricter penalty term [i.e., for $n \geq 8$, the BIC penalty ($k \ln n$) is greater than the AIC penalty ($2k$)] and will thus discriminate more strongly against time-varying recruitment parameters.} The summarized results of the model selection procedure are given in Table S3.

ΔR_{MAX} and ΔR^k_{MAX}. The dynamic linear regression analysis yields time series of recruitment parameters R^i_{MAX}, and ΔR^i_{MAX} for 262 fish populations (now using i to denote an individual stock). We then summarize the trend using a linear slope based on least squares regression

$$R^i_{MAX} = b^i_0 + b^i_1 t + e^i_t,$$

where b^i_0 is the intercept of the linear regression for stock i, b^i_1 is the slope multiplied by time index t, and e^i_t is the regression error. To standardize the rate of change in recruitment, we define

$$\Delta R^i_{MAX} = \frac{b^i_1}{\max(R^i_{MAX})} * 10\,\text{years}.$$

which represents the rate of change per decade (10 years) as a percent relative the historical maximum of R^i_{MAX}. To estimate the uncertainty in ΔR^i_{MAX} according to the uncertainty in the estimated time-varying recruitment parameters, we used a bootstrap resampling scheme as follows. (i) Sample from the uncertainty distribution of the inferred time-varying recruitment parameters to compute bootstrapped time series of R^i_{MAX}. (ii) Compute the standardized linear slope ΔR^i_{MAX} from the bootstrapped R^i_{MAX} series. (iii) Repeat 500 times. This procedure yields bootstrapped distributions of ΔR^i_{MAX} with uncertainty determined by the uncertainty in the inferred recruitment parameters. Due to the nonlinearity in R_{MAX}, we use the median and median absolute deviation (MAD) as summary statistics for robustness.

To combine the results of the individual trend analyses, we perform a random effects meta-analysis at the taxonomic, regional, and global scales. For any particular grouping, the random-effects model is written

$$\Delta R^i_{MAX} = \Delta R^k_{MAX} + \vartheta^i + \varphi^i,$$

where ΔR^i_{MAX} is the estimated linear slope of R_{MAX} for stock i, ΔR^k_{MAX} is the overall mean ΔR_{MAX} for in the group, ϑ^i is the deviation of the observed ΔR^i_{MAX} from the true ΔR^i_{MAX}, and φ^i is the deviation of the true ΔR^i_{MAX} from ΔR^k_{MAX}. In the estimation, weights are applied according to the inverse variance of the

bootstrap distribution of ΔR^i_{MAX}. The meta-analysis model was implemented in the R package *rmeta* (32). All meta-analytic results for LMEs and taxa are given in *SI Appendix*.

Sensitivity Analyses.

Sensitivity of R_{MAX} trends to alternative forms of density dependence. The Ricker function is only one of several possible parameterizations for the recruitment function. Other common recruitment functions include the Beverton–Holt model, $R_t = \alpha[\beta/(1+\beta B_{t-\tau})]$, or the more general three-parameter Shephard curve, $R_t = \alpha(1-\gamma\beta B_{t-\tau})^{1/\gamma}$, both of which vary in their representation of density dependence. Several studies (35–37) have found that the Ricker model is most robust to biases introduced by both observation error and model misspecification. These results motivated our use of the Ricker function in the paper. However, we also tested the sensitivity of our results to the shape of density dependence by applying the generalized Ricker function (35), which approximates the behavior of the above models through the inclusion of the shape parameter γ

$$R_t = \alpha B_{t-\tau} e^{-(\beta B_{t-\tau})^{\gamma}}.$$

We set $\gamma = 0.5$, 0.75, 1.25, and 1.5 to simulate the range of density-dependent behaviors from very weak ($\gamma = 0.5$) to highly overcompensatory ($\gamma = 1.5$). See Fig. S2 for depictions of the various forms of density dependence. Note that $\gamma = 1$ recovers the Ricker model. We found that the quantity ΔR^i_{MAX} was generally independent of the shape parameter γ (Figs. S3 and S4) and thus independent of the form of density dependence in the recruitment function. The individual recruitment parameters α and β changed in relative magnitude with γ (Fig. S3) in a way that resulted in α and β parameters closer to zero with increasing γ. However, the standardized slopes remained constant (Fig. S4) because as γ increases, the parameter is vertically translated on the y axis, altering the y intercept, but leaving the slope unchanged. This transformation resulted in constant ΔR^i_{MAX} across all values of γ.

Sensitivity of R_{MAX} trends to parameterization of Q. The BIC model selection algorithm was used to choose the appropriate structure of the covariance matrix **Q**, which determined whether recruitment parameters varied in time. We tested the sensitivity of R^i_{MAX} and ΔR^i_{MAX} to the alternate parameterizations of **Q** by repeating the model selection two times under a restricted set of possible **Q** parameterizations: (*i*) static stock-recuit vs. time-varying α; and (*ii*) static stock-recruit vs. time-varying β. We then took each set of results and repeated the estimation procedure for R^i_{MAX} and ΔR^i_{MAX}. Results indicated that the distribution of ΔR^i_{MAX} was relatively insensitive to whether **Q** was parameterized to represent time-varying α or β. The magnitudes and relative number of stationary vs. time-varying stock-recruit relationships also remained similar, as well as the magnitudes of ΔR^i_{MAX}. The main difference was that time-varying α tended to produce larger SEs for ΔR^i_{MAX}. The results of this analysis are presented in Fig. S5.

Sensitivity to an alternative definition of recruitment capacity. For some heavily depleted stocks, or those exhibiting extremely weak density dependence, the majority of the historically observed biomass may be below the biomass that produces maximum recruitment; therefore, R_{MAX} may not be a practical metric for management. To test the robustness of trends to the specific definition of recruitment capacity, we repeated the trend analysis with an alternative definition; specifically, recruitment evaluated at the median observed biomass, $R[B = median(B)]$ (Fig. S6). We found that $\Delta R[B = median(B)]$ correlated very strongly with ΔR_{MAX} at the regional and global scales, with correlations of 0.85 and 0.92, respectively. Magnitudes of $\Delta R[B = median(B)]$ were slightly smaller than ΔR_{MAX} but were generally estimated with smaller bootstrap resampled variances so resulting in very similar P values at the global and regional scales.

Analysis over the years 1980:2000. To test the sensitivity of our results to variable time series length, we repeated the time-varying recruitment analysis by subsetting time series for the period 1980:2000 and excluded stocks that do not cover this period. This subset excluded six stocks from the analysis. The scatterplot between ΔR^i_{MAX} using the full time series and ΔR^i_{MAX} calculated for the period 1980:2000 is given in Fig. S7. The results indicate a high correlation of 0.82 indicating a robustness in the overall trends that is not driven by the longer time series.

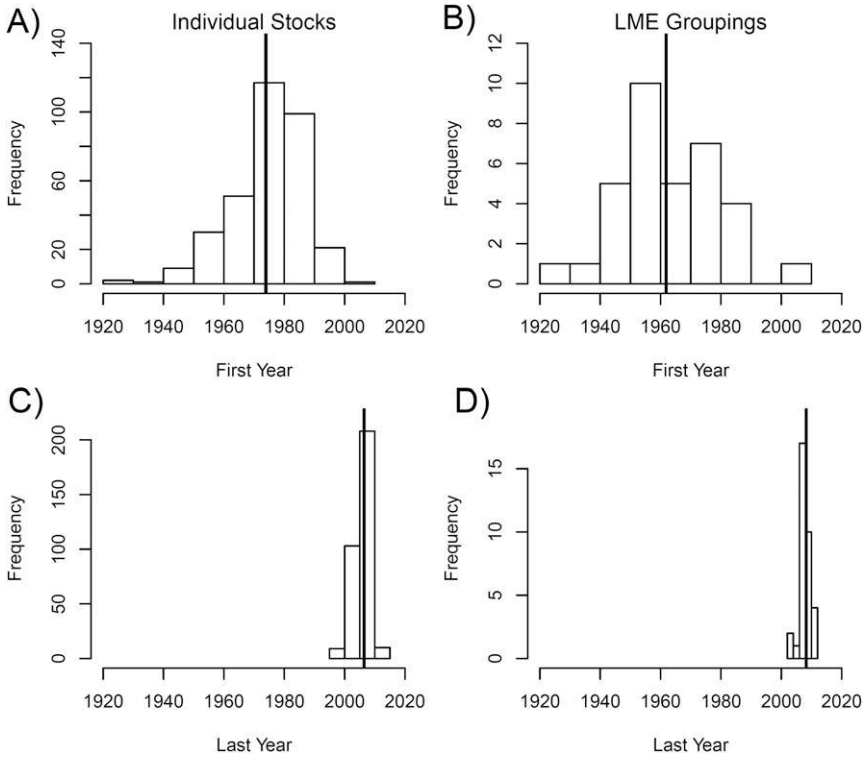

Fig. S1. Frequency distribution of start and end dates of time series analysis in this study. *A* and *B* give the distribution of start dates for individual stocks and LME groupings, respectively, and *C* and *D* give end dates.

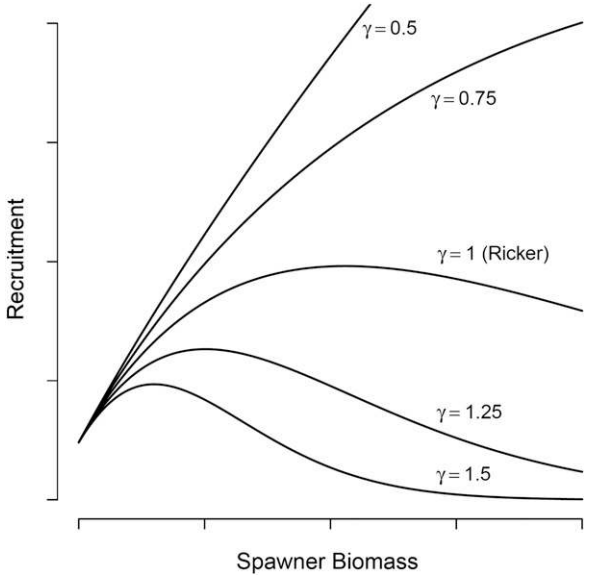

Fig. S2. The generalized Ricker model and alternate forms of density dependence. The shape parameter γ in the generalized Ricker model has a strong effect on the form of density dependence in the stock-recruit relationship. Increasing values of γ lead to stronger density-dependence feedback, and as $\gamma \to 0$, the generalized Ricker describes a linear relation between stock and recruitment with slope α.

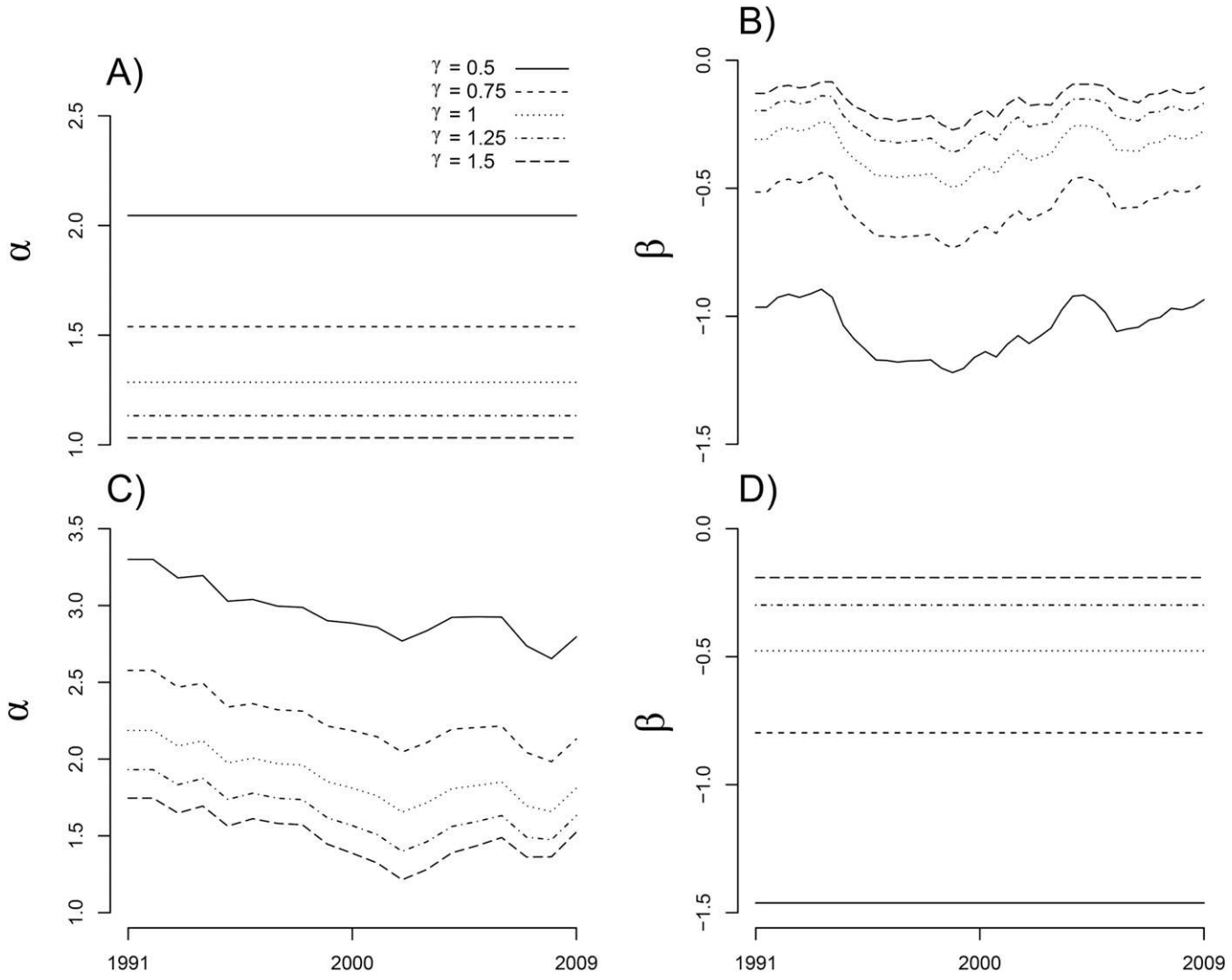

Fig. S3. Effect of γ transformation on recruitment parameters α and β. As examples, *A* and *B* give the estimated recruitment parameters for Peruvian anchoveta (north-central Peru) and *C* and *D* give recruitment parameters for Southern blue whiting (southern Argentina). The two stocks exhibited time-varying α and β, respectively, according to model selection. The reader should note that varying γ affects the magnitude of the parameters, but not the time variability. As a result, the standardized slopes (when expressed in terms of % relative to historical maximum) remain constant and independent of γ.

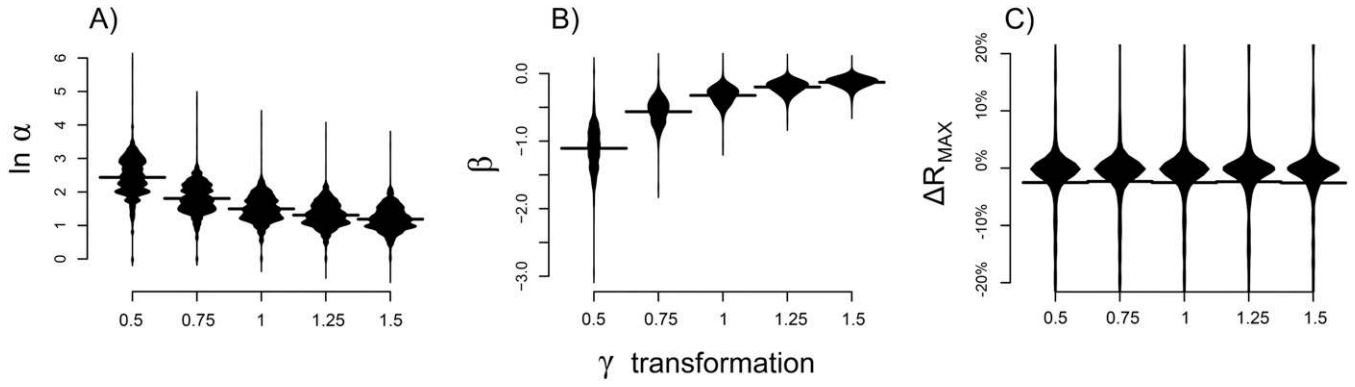

Fig. S4. Sensitivity analysis. To test the sensitivity of ΔR_{MAX} to alternate forms of the stock-recruit relationship, the dynamic regression models were applied to the generalized Ricker model using prescribed values for the shape parameter γ (Figs. S2 and S3 and *SI Methods*). (*A* and *B*) Distribution and median of α and β estimates under each value of γ (note $\gamma = 1$ recovers the traditional Ricker model used in this study). (*C*) Distribution of the standardized linear slopes ΔR_{MAX} under the γ transformations. These results imply that the ΔR_{MAX} quantity (when expressed in terms of % relative to historical maximum) was independent of the form of density-dependence in the generalized Ricker model.

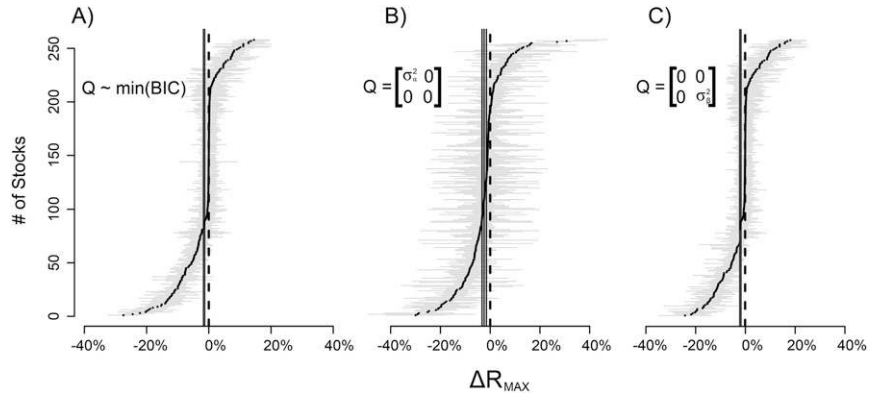

Fig. S5. Sensitivity of ΔR_{MAX} to model selection and specification. We tested the sensitivity of individual ΔR_{MAX} to the parameterization of the covariance matrix of the recruitment parameters **Q**. (*A*) Distribution of ΔR_{MAX} (and SE) when choosing the elements of **Q** according to BIC model selection. (*B*) Distribution ΔR_{MAX} when performing model selection between static stock-recruit vs. time-varying α. (*C*) ΔR_{MAX} for model selection between static stock-recruit and time-varying β. These results imply that maximum recruitment potential was relatively independent of whether we allowed α or β to vary.

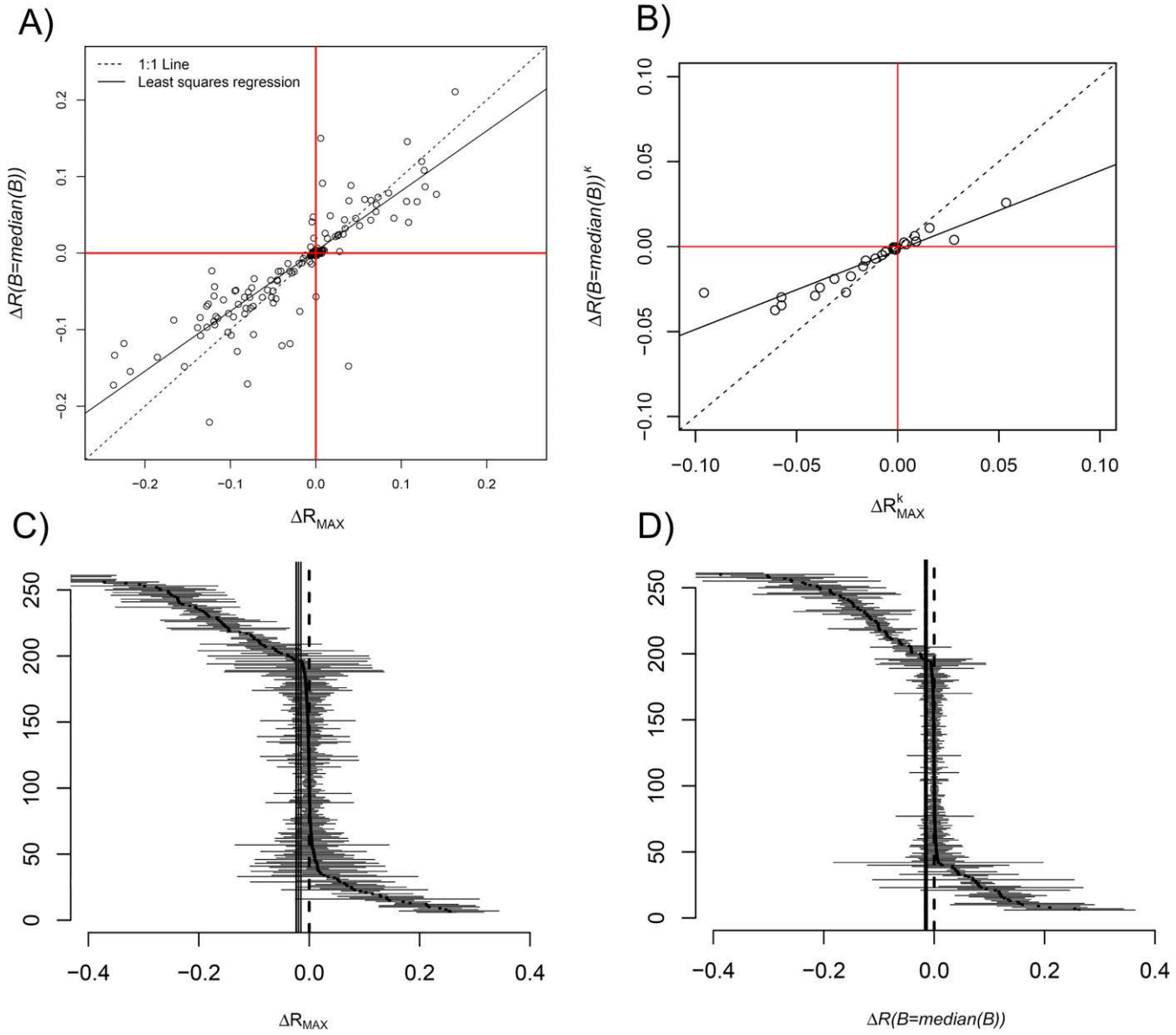

Fig. S6. Comparison of ΔR_{MAX} with an alternative recruitment metric $\Delta R[B = median(B)]$. (*A* and *B*) Scatterplot between slopes of recruitment capacity (ΔR_{MAX}) and recruitment evaluated at median observed biomass ($\Delta R[B = median(B)]$) for individual stocks and LME regions, respectively. The correlation between the two respective metrics was $r = 0.85$ and $r = 0.92$. Note that the regression line has a smaller slope than the 1:1 line, in both cases indicating that the ($\Delta R[B = median(B)]$) metric resulted in slightly smaller magnitudes. (*C* and *D*) Global meta-analysis results for the respective metrics ΔR_{MAX} and ($\Delta R[B = median(B)]$). The dashed line at zero represents no effect and the solid black lines give the bands of the 95% meta-analytic CIs. Notice that ΔR_{MAX} gives a slightly larger effect size with wider confidence limits, which results in similar statistical significance.

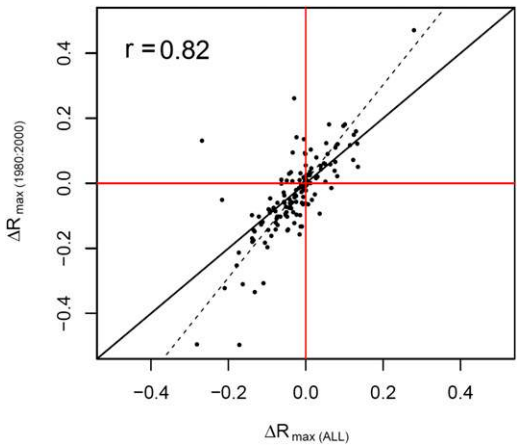

Fig. S7. Scatterplot between ΔR_{MAX} using the full time series (denoted $\Delta R_{MAX(all)}$ and ΔR_{MAX} calculated for the period 1980:2000 (denoted $\Delta R_{MAX(1980:2000)}$). The results indicate a high correlation indicating robustness in the trends to the length of the time series analyzed.

Other Supporting Information Files

SI Appendix (PDF)
Table S1 (DOCX)
Table S2 (DOCX)
Table S3 (DOCX)